Cellular/Molecular

Reversible Suppression of Glutamatergic Neurotransmission of Cerebellar Granule Cells *In Vivo* by Genetically Manipulated Expression of Tetanus Neurotoxin Light Chain

Mutsuya Yamamoto,[1,2,3] Norio Wada,[2] Yasuji Kitabatake,[3] Dai Watanabe,[3] Masayuki Anzai,[4] Minesuke Yokoyama,[5] Yutaka Teranishi,[5] and Shigetada Nakanishi[2,3]

[1]Mitsubishi Pharma Corporation, Discovery Technology Laboratory, Yokohama, 227-0033, Japan, [2]Department of Molecular and System Biology, Kyoto University Graduate School of Biostudies, Kyoto, 606-8501, Japan, [3]Department of Biological Sciences, Kyoto University Faculty of Medicine, Kyoto, 606-8501, Japan, [4]GenCom Corporation, Machida, 194-8511, Japan, and [5]Mitsubishi Kagaku Institute of Life Sciences, Machida, 194-8511, Japan

We developed a novel technique that allowed reversible suppression of glutamatergic neurotransmission in the cerebellar network. We generated two lines of transgenic mice termed Tet and TeNT mice and crossed the two transgenic lines to produce the Tet/TeNT double transgenic mice. In the Tet mice, the tetracycline-controlled reverse activator (rtTA) was expressed selectively in cerebellar granule cells by the promoter function of the $GABA_A$ receptor $\alpha 6$ subunit gene. In the TeNT mice, the fusion gene of tetanus neurotoxin light chain (TeNT) and enhanced green fluorescent protein (EGFP) was designed to be induced by the interaction of doxycycline (DOX)-activated rtTA with the tetracycline-responsive promoter. The Tet/TeNT mice grew normally even after DOX treatment and exhibited a restricted DOX-dependent expression of TeNT in cerebellar granule cells. Along with this expression, TeNT proteolytically cleaved the synaptic vesicle protein VAMP2 (also termed synaptobrevin2) and reduced glutamate release from granule cells. Both cleavage of VAMP2/synaptobrevin2 and reduction of glutamate release were reversed by removal of DOX. Among the four genotypes generated by heterozygous crossing of Tet and TeNT mice, only Tet/TeNT mice showed DOX-dependent reversible motor impairments as analyzed with fixed bar and rota-rod tests. Reversible suppression of glutamatergic neurotransmission thus can be manipulated with spatiotemporal accuracy by DOX treatment and removal. These transgenic mice will serve as an animal model to study the cerebellar function in motor coordination and learning.

Key words: **transgenic mouse; $GABA_A$ receptor; tetanus neurotoxin; tetracycline-inducible system; cerebellum; granule cell; VAMP2; glutamatergic transmission**

Introduction

One useful approach to understanding mechanisms underlying information processing and integration in the neural circuit involves inactivating specific neurons in the neural network. This approach has been used effectively in *Drosophila* and *Caenorhabditis elegans* (*C. elegans*) in some cases by reversibly inactivating a subset of neurons (Sweeney et al., 1995; Dubnau et al., 2001; McGuire et al., 2001; White et al., 2001). In mammals, the cell targeting that allows selective ablation of a particular cell type within the network has been developed by genetically manipulating techniques (Nirenberg and Cepko, 1993; Kobayashi et al., 1995; Watanabe et al., 1998; Gogos et al., 2000). This technology has clarified mechanisms underlying development, information processing and integration, and behaviors but also often has led to adaptive and compensatory changes in the neural function (Watanabe et al., 1998; Kaneko et al., 2000). The technology that allows reversible suppression of a specific neuronal activity in mammals is desired but still is limited (Steele et al., 1998).

Neurotransmitter is stored in and released from synaptic vesicles by Ca^{2+}-regulated exocytosis (Südhof, 1995). VAMP2 (also known as synaptobrevin) is a core protein of synaptic vesicles (Baumert et al., 1989; Elferink et al., 1989; Archer et al., 1990; Söllner et al., 1993a,b) and is required for synaptic vesicle exocytosis (Südhof, 1995; Schoch et al., 2001). This vesicle protein is a target of tetanus neurotoxin. The light chain of tetanus neurotoxin (TeNT) proteolytically cleaves VAMP2 between Gln-76 and Phe-77 and impairs synaptic vesicle exocytosis (Link et al., 1992; Schiavo et al., 1992). The proteolytic inactivation of VAMP2 by genetic manipulation with TeNT thus would be approached to suppress synaptic transmission in the neural network. So that a temporally regulated expression of a transgene *in vivo* could be achieved, the tetracycline-controlled reverse transactivator (rtTA) system was developed (Gossen et al., 1995). In this system, rtTA, when bound to tetracycline or its derivative

Received April 23, 2003; revised June 3, 2003; accepted June 5, 2003.

This work was supported in part by research grants from the New Energy and Industrial Technology Development Organization and the Ministry of Education, Science, and Culture of Japan. We thank Shinichi Nakamura for a gift of *Clostridium tetani* (strain KZ1174), Mitsuaki Nishibuchi for a culture of *C. tetani*, and Masami Takahashi for a gift of rabbit polyclonal VAMP2 antibody. We also thank Hirohito Nishino, Tomoyuki Furuyashiki, Takayuki Nakagawa, Masamichi Satoh, and Takehisa Ishii for invaluable advice.

Correspondence should be addressed to Mutsuya Yamamoto, Mitsubishi Pharma Corporation, Discovery Technology Laboratory, 1000, Kamoshida-cho, Aoba-ku, Yokohama, 227-0033, Japan. E-mail: Yamamoto.Mutsuya@mf.m-pharma.co.jp.

 0270-6474/03/236759-09$15.00/0

doxycycline (DOX), activates the expression of a transgene via interaction with the tetracycline-responsive element (TRE). The genetically manipulated expression of TeNT with the rtTA system thus would confer inducible and reversible suppression of synaptic transmission *in vivo* by DOX-dependent cleavage of VAMP2.

The cerebellar cortex forms an array of defined neural networks consisting of mossy fibers, granule cells, parallel fibers, and Purkinje cells (Ito, 1984). Granule cells, a major cell population of the cerebellar cortex, transmit excitatory inputs to Purkinje cells via glutamatergic neurotransmission. It has been reported that the 5′-upstream genomic region of $GABA_A$ receptor $\alpha6$ subunit (GABA-$\alpha6$) directs a selective expression of the β-galactosidase reporter gene in cerebellar granule cells (Bahn et al., 1997). We combined the GABA-$\alpha6$-directed expression of rtTA with the DOX/rtTA-controlled TeNT system and investigated reversible TeNT-mediated suppression of glutamatergic transmission in cerebellar granule cells. Here we report that the DOX-dependent expression of TeNT reversibly interferes not only with glutamate release from granule cells but also with coordinate control of motor movement.

Materials and Methods

Generation of Tet and TeNT mice. All procedures for animal treatments and cultures of *Clostridium tetani* were performed according to the guidelines of Kyoto University Faculty of Medicine. The 409 bp exon 1 fragment of the GABA-$\alpha6$ gene (residues 1240–1648; GenBank accession number AJ222970) was amplified from the genomic DNA of C57BL/6J mice by PCR. A mouse genomic DNA containing the GABA-$\alpha6$ gene was screened from the mouse bacterial artificial chromosome (BAC) filter (Release II, Genome Systems, St. Louis, MO) by the GABA-$\alpha6$ probe. The 7.2 kilobase pair (kbp) *Sph*I–*Afl*II fragment containing the 5′-upstream region and exons 1–8 of the GABA-$\alpha6$ gene was isolated from the BAC DNA. The rtTA cDNA followed by the SV40 late polyadenylation signal (SV40pA) was isolated from the pTet-On vector (Clontech, Palo Alto, CA), and a *Not*I site was added to the 3′ end of the SV40pA sequence. The *Sph*I site in the rtTA cDNA was replaced with the GCACGC sequence without changing its coding amino acid sequence. The internal ribosome entry site (IRES) of encephalomyocarditis virus (Jackson et al., 1990) was linked to the rtTA sequence in which the 11th ATG within the IRES sequence was used as a translation initiation site of the rtTA gene. An *Afl*II site and the termination codons in the three reading frames were appended at the 5′ end of the IRES sequence. The 7.2 kbp *Sph*I–*Afl*II fragment containing the GABA-$\alpha6$ gene was ligated to the 2.1 kbp *Afl*II–*Not*I fragment containing the IRES, rtTA, and SV40pA sequences and subcloned into the pUC18 vector.

The EGFP cDNA (residues 679-1395) was amplified from the pd1EGFP-N1 vector (Clontech). A *Sac*II site and the Kozak sequence (Kozak, 1986) were added to the 5′ end of the EGFP cDNA, and a *Mlu*I site was added to its 3′ end. The DNA fragment encoding TeNT (residues 281-1651, GenBank accession number X04436) was isolated from boiled supernatants of cultured *Clostridium tetani* (strain KZ1174, a gift from Dr. Nakamura, Kanazawa University School of Medicine, Kanazawa, Japan). A *Mlu*I site and a *Not*I site were added to the 5′ and 3′ ends of the TeNT sequence, respectively. The PEST sequence (proline, glutamic acid, serine, and threonine) of ornithine decarboxylase (residues 1402–1524) (Li et al., 1998) was prepared from the pd1EGFP-N1 vector. A *Not*I site and one additional nucleotide (T) were added to the 5′ end of the PEST sequence to link the PEST sequence in-frame to the TeNT sequence, and a *Xba*I site was added to its 3′ end. The multiple restriction sites in the pTRE2 vector (Clontech) intervene between the tetracycline-responsive element/the cytomegalovirus promoter (TRE/CMV) and the β-globin intron/polyadenylation signal. The pTRE2 vector was cleaved at the multiple restriction sites with *Sac*II and *Xba*I sites, and the *Sac*II–*Mlu*I fragment containing the EGFP sequence and the *Mlu*I–*Xba*I fragment containing the TeNT and PEST sequences were inserted into the *Sac*II and *Xba*I sites of the pTRE2 vector. The 3.9 kbp *Xho*I–*Sap*I fragment of the TeNT transgene (see Fig. 1*B*) and the 9.3 kbp *Sph*I–*Not*I fragment of the Tet transgene (see Fig. 1*C*) were purified from 1% low-melting agarose gel (Invitrogen, San Diego, CA) in 0.5× TBE (0.045 M Tris-borate and 0.001 M EDTA). The purified fragments were injected into the pronucleus of fertilized eggs of C57BL/6J mice (Hogan et al., 1994).

DOX treatment. DOX was administered with pellets containing 6 mg/gm DOX (BioServe Biotechnologies, Laurel, MD) and drinking water containing 2 mg/ml DOX (Sigma, St. Louis, MO) and 10% sucrose. DOX-containing water was maintained in dark bottles to prevent degradation of DOX and changed three times a week. Unless otherwise stated, animals at ages of 4–5 weeks were treated or untreated with DOX for 14 d and termed DOX-treated and DOX-untreated mice, respectively. Animals at the same age also were treated with DOX for 14 d, followed by 21 d without DOX treatment, and termed DOX-withdrawn mice.

RNA blotting and in situ *hybridization analysis.* RNA blotting was performed with a digoxigenin (DIG)-labeled rtTA cRNA probe in DIG Easy Hyb solution (Roche Diagnostics, Pleasanton, CA) as described previously (Yamamoto et al., 1999). Hybridization signals were detected by using the DIG-luminescent detection kit (Roche Diagnostics). *In situ* hybridization of brain sections (10 μm in thickness) was performed as described previously (Akazawa et al., 1994). A 648 bp rtTA DNA fragment (residues 369-1016) and a 358 bp EGFP DNA fragment (residues 679-1036) were obtained by PCR from the pTet-On vector and the pd1EGFP-N1 vector, respectively, and used for hybridization analysis.

Immunohistochemistry and immunoblotting. Immunohistochemistry was performed with the avidin-biotinylated peroxidase complex (ABC) method or double-immunofluorescence method as described previously (Ohishi et al., 1994). On double immunostaining, VectaShield (Vector Laboratories, Burlingame, CA) was used to prevent immunofluorescence bleaching, and immunostained sections were detected under confocal laser scanning microscope (LSM510 META, Zeiss, Oberkochen, Germany). For immunoblotting, the tissues were homogenized with a plastic pestle in 10 volumes of PBS containing 2% SDS, 2 mM EDTA, and a protease inhibitor mixture (Complete, Mini, EDTA-free, Roche Diagnostics). After being boiled for 5 min, the lysates were centrifuged at 15,000 rpm for 5 min, and supernatants were collected. The supernatant containing 8–80 mg of protein was electrophoresed on 4–20% gradient or 15% polyacrylamide gels containing 0.1% SDS and transferred to the Immobilon-P membrane (Millipore, Bedford, MA). Immunodetection was performed as described previously (Yamamoto et al., 2002). The primary antibodies used were as follows: mouse monoclonal antibodies against calbindin D-28 (1:3000) and parvalbumin (1:5000) (both from Sigma); syntaxin (1:10,000; Upstate Biotechnology, Lake Placid, NY), β-tubulin (1:200; Chemicon, Temecula, CA); PSD-95 (1:2000), munc13 (1:250), and munc18 (1:25,000) (all from Transduction Laboratories, Lexington, KY); rabbit polyclonal antibodies against GFP (1:2000; Molecular Probes, Eugene, OR); VAMP2 (1:12,500; a gift from Dr. Takahashi, Mitsibushi Kagaku Institute of Life Sciences, Machida, Japan) (Oho et al., 1995); cellubrevin (1:4000; Abcam, Cambridge, UK), $GABA_A\alpha1$ (1:10,000) and NR2A (1:2000) (both from Upstate Biotechnology); $GABA_A\alpha6$ (1:2000), NR2C (1:2500), and NSF (1:5000) (all from Chemicon); rab3A (1:1000; Santa Cruz Biotechnology, Santa Cruz, CA); and goat polyclonal antibodies against synaptotagmin 2 (1:100), synaptophysin (1:100), and SNAP25 (1:900) (all from Santa Cruz Biotechnology). The secondary antibodies used were as follows: HRP-conjugated donkey anti-goat IgG, HRP-conjugated goat anti-mouse IgG, HRP-conjugated goat anti-rabbit IgG (all from Santa Cruz Biotechnology), biotinylated goat anti-rabbit IgG (Vector Laboratories), Alexa Fluor 488-conjugated goat antiserum against rabbit IgG, and Alexa Fluor 594-conjugated goat antiserum against mouse IgG (both from Molecular Probes).

Measurement of glutamate release. A cerebellum was sliced with a 300 μm cube by using a McIlwain tissue chopper (Mickle Laboratory Engineering, Gomshall, UK) (Miyamoto et al., 2001). The white matter was removed from the slices as much as possible under a stereoscopic microscope (Zeiss). One-fifth of the slices was loaded on a glass fiber filter (GF/B, Whatmann, Maidstone, UK) in a superfusion chamber (Warner Instruments, Grand Haven, MI) and superfused at 37°C with a low-KCl Krebs' buffer [containing (in mM): 118 NaCl, 3.5 KCl, 1.25 $CaCl_2$, 1.2

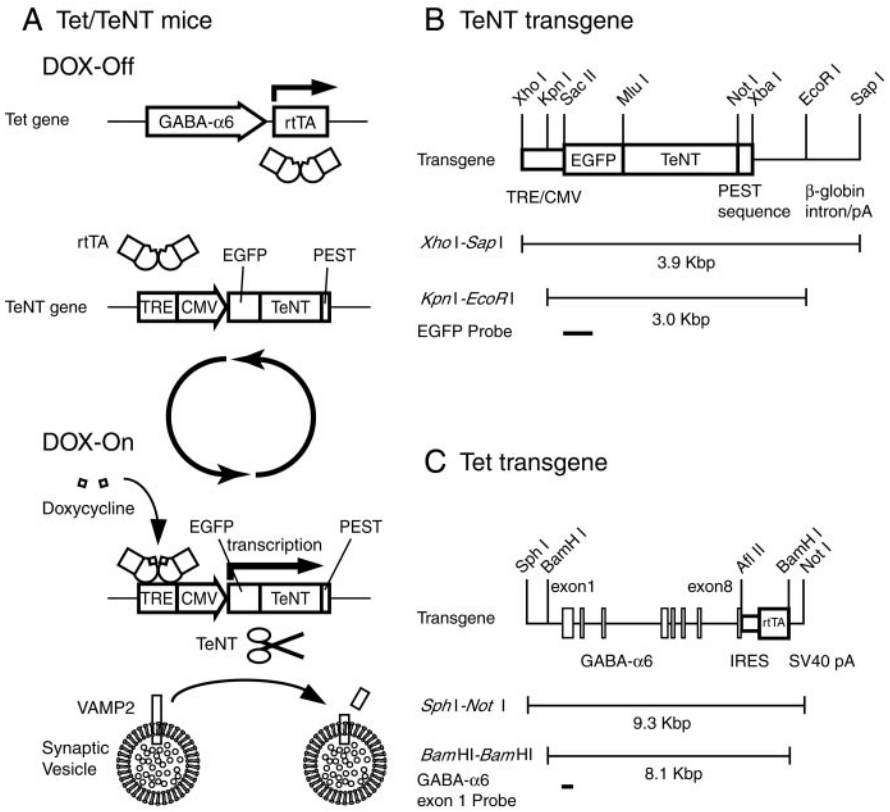

Figure 1. Strategy for DOX-dependent reversible suppression of glutamatergic transmission from cerebellar granule cells *in vivo*. *A*, Scheme of reversible expression of TeNT in cerebellar granule cells. In the Tet/TeNT double transgenic mice, the expression of rtTA of the Tet transgene is directed by the GABA-α6 promoter and thus confined to cerebellar granule cells. The expression of the TeNT transgene is controlled by the TRE/CMV promoter so that TeNT is expressed only when DOX binds to rtTA and activates the TRE/CMV promoter. Consequently, under the DOX-free condition (DOX-Off), rtTA expressed in cerebellar granule cells remains inactive, and, when DOX is administered, DOX binds to rtTA and induces the TeNT expression in cerebellar granule cells (DOX-On). TeNT in turn cleaves VAMP2 and impairs glutamate release from granule cells. When DOX is withdrawn, rtTA becomes inactive, and newly synthesized VAMP2 restores glutamatergic transmission. *B*, A schematic structure of the TeNT transgene. The 3.9 kbp *Xho*I–*Sap*I fragment used as the TeNT transgene consists of the TRE/CMV promoter, the fusion gene of EGFP and TeNT, and the downstream β-globin genomic sequence containing polyadenylation signal (β-globin intron/pA); the PEST sequence is attached at the C terminus of TeNT. When genomic DNA of the TeNT mice is digested with *Kpn*I and *Eco*RI, the EGFP probe gives rise to a hybridization signal of the 3.0 kbp *Kpn*I–*Eco*RI fragment derived from the transgene. *C*, A schematic structure of the Tet transgene. The 9.3 kbp *Sph*I–*Not*I used as the Tet transgene consists of the genomic sequence containing the 5′-upstream region and exons 1–8 of the GABA-α6 gene, followed by IRES, the rtTA cDNA, and the SV40pA. When genomic DNA of the Tet mice is digested with *Sph*I and *Bam*HI, the GABA-α6 exon 1 probe gives rise to hybridization signals of the 8.1 kbp *Bam*HI fragment derived from the transgene and the 14 kbp *Bam*HI–*Sph*I fragment derived from the mouse genomic DNA (data not shown). In *B* and *C*, only restriction sites used for transgene construction and Southern analysis are indicated.

$MgSO_4$ 1.2 KH_2PO_4, 25 $NaHCO_3$, and 11.5 D-glucose] with a flow rate of 0.5 ml/min under continuous aeration with 95% O_2/5% CO_2 (Lonart et al., 1998). After superfusion with the low-KCl Krebs' buffer for 64 min (32 ml), a fraction (1 ml) was collected continuously from 64 to 78 min. During fractionation, a high-KCl (25 mM) Krebs' buffer was superfused from 70 to 72 min to depolarize slices. Then the slices were removed from a glass fiber and solubilized with 0.1 M perchloric acid (1 ml; Nacalai Tesque, Kyoto, Japan). The solubilized extract was diluted 20 times in a mobile phase and passed through an ultrafiltrate membrane with cutoff of molecular size >10,000 Da (UFC3 LGC00, Millipore). A mobile phase was composed of 50 mM NH_4Cl-NH_4OH, pH 7.2, and 250 mg/l hexadecyltrimethylammonium bromide (Nacalai Tesque). The concentrations of glutamate in the first 32 ml fraction and the subsequent fraction (1 ml each) of collected superfusions and solubilized slice extracts were determined by HPLC according to the procedures described by Yao et al. (1995). The HPLC system (HTEC-500, EiCOM, Kyoto, Japan) consisted of a pre-column (CH-GEL, EiCOM), a column (E-GEL, EiCOM), a glutamate oxidase-immobilized reactor (E-ENZ 3 × 4 mm, EiCOM), and an electrochemical detector equipped with a platinum electrode (WE-PT, EiCOM). The concentration of total glutamate was calculated by summing the amounts of glutamate released in the superfusions and that of slice extracts.

Fixed bar and rota-rod tests. Both analyses were conducted as described previously (Kadotani et al., 1996). The fixed bar consisted of a wooden bar (6 mm in width and 70 cm in length) that was held horizontally on both ends 40 cm above the ground. A mouse, which weighed >14 gm, was placed on the center of the bar, and the time it remained on the bar was measured. After the mouse reached the end of the bar, the measurement was suspended temporally, the mouse was replaced on the center position, and measurement was resumed. A maximum of 60 sec was allowed per animal. The rota-rod (Ugo Basile, Comerio, Italy) consisted of a gritted plastic roller (4 cm in diameter). A mouse was placed on the rota-rod rotating at 35 rpm. Testing was performed with six sessions of three trials per session; three sessions were conducted per day. The staying time of each trial in one session was summed and defined as a score of each session.

Results

Experimental design for reversible control of glutamatergic transmission *in vivo*

Reversible control of glutamatergic synaptic transmission *in vivo* was designed by generating two lines of transgenic mice, termed Tet and TeNT mice (Fig. 1*A*). In the TeNT transgene the TRE was attached consecutively to the CMV promoter and placed upstream of the fusion gene of EGFP and TeNT, followed by polyadenylation signals of the β-globin gene (Fig. 1*B*). The PEST sequence of mouse ornithine decarboxylase also was attached to the C terminus of TeNT to facilitate degradation of the EGFP/TeNT protein (Li et al., 1998). It has been reported that the 7.2 kbp mouse genomic fragment containing the 5′-upstream sequence and exons 1–8 of the $GABA_A$ receptor α6 subunit gene (GABA-α6) is capable of directing selective expression of the β-galactosidase transgene in cerebellar granule cells (Bahn et al., 1997). According to this report, we constructed the Tet transgene that consisted of the truncated GABA-α6 gene, the IRES of encephalomyocarditis virus (Jackson et al., 1990), the rtTA-encoding cDNA, and the SV40pA in this order (Fig. 1*C*). This construct was designed to allow a specific expression of bicistronic mRNA in cerebellar granule cells. In addition, a stop codon was attached at the three reading frames of the GABA-α6 exon 8 sequence. As a consequence, IRES should enable the bicistronic mRNA to be translated into the truncated form of $GABA_A$ receptor α6 subunit and rtTA (Fig. 1*C*). We then generated double transgenic mice termed Tet/TeNT mice by mating the Tet mice with the TeNT mice. In the Tet/TeNT mice rtTA is kept inactive under the DOX-free conditions (DOX-Off). When animals are treated with DOX (DOX-On), DOX binds to rtTA and selectively induces the TRE-regulated expression of the EGFP/TeNT fusion gene in cerebellar

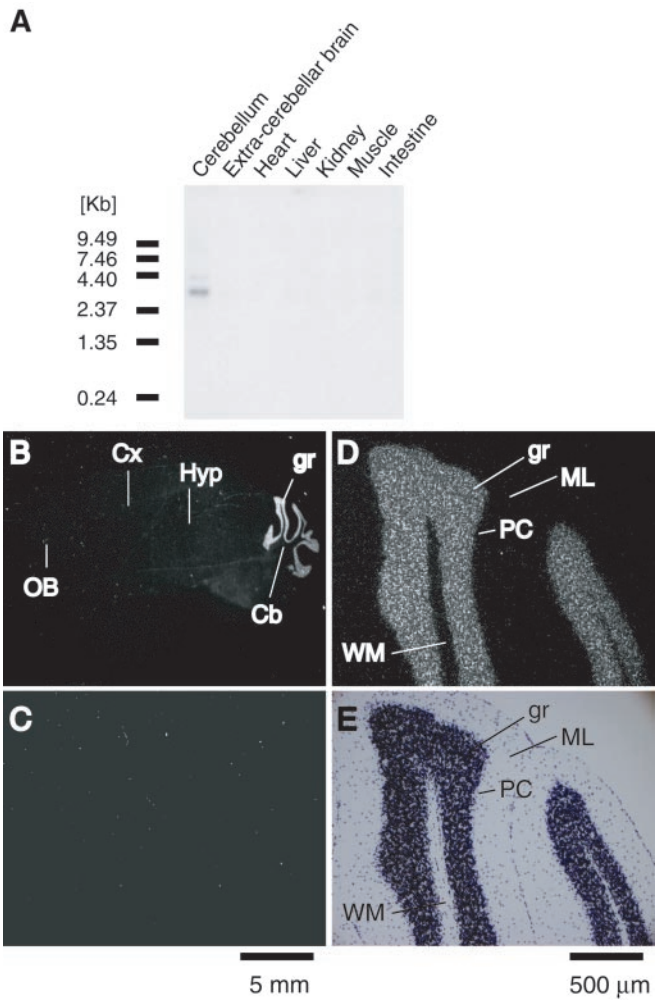

Figure 2. Analysis of rtTA mRNA expression. *A*, RNA blotting of various tissues of the Tet mice with rtTA cRNA probe. *B, C*, Dark-field images of *in situ* hybridization analysis of sagittal sections of the Tet (*B*) and wild-type (*C*) mice with rtTA cRNA probe. OB, Olfactory bulb; Cx, cerebral cortex; Hyp, hippocampus; Cb, cerebellum; gr, granule cell. *D, E*, A magnified view of dark-field (*D*) and bright-field (*E*) images of *in situ* hybridization analysis of a cerebellar section. The section in *E* was counterstained with crystal violet, showing no hybridization signals in Purkinje cells. PC, Purkinje cell; ML, molecular layer; WM, white matter.

granule cells (Fig. 1*A*). Then removal of DOX returns rtTA to the DOX-Off state and turns off the expression of the EGFP/TeNT (Fig. 1*A*). Under this design, the expression of TeNT not only should be confined to cerebellar granule cells but also should be controlled conditionally by the administration of DOX. Once TeNT is induced, it could cleave VAMP2 and suppress glutamatergic transmission from granule cells. This suppression would be reversed by withdrawal of DOX. Therefore, the strategy we adopted here should allow reversible control of glutamatergic transmission from granule cells in a DOX-dependent manner.

Restricted expression of GABA-α6/rtTA mRNA in cerebellar granule cells

Ten independent founders of the Tet mice were generated with the integrated copy number from 1 to ~20. Northern blot analysis with a rtTA probe gave rise to a transcript with ~3 kilonucleotides in the cerebellum of all 10 transgenic lines (Fig. 2*A*). This size was consistent with the calculated size of the transgene mRNA that undergoes faithful splicing and polyadenylation (Fig. 1*C*). Among the 10 founders, line 620 with four copies of the

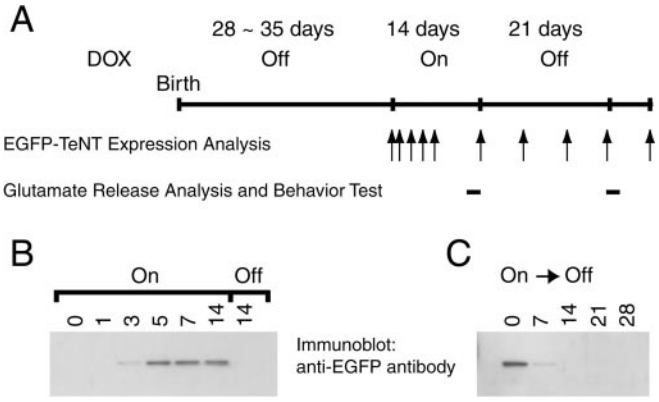

Figure 3. Schedule of DOX treatment and analysis of DOX-dependent expression of TeNT in the cerebellum of the Tet/TeNT mice. *A*, The time schedule for DOX treatment and an analysis of TeNT expression, glutamate release, and animal behaviors are indicated. On, DOX-treated; Off, DOX-untreated or DOX-withdrawn. *B*, Immunoblot analysis of EGFP/TeNT in cerebellar lysates before and after DOX treatment; the mice at the top right lane were handled similarly but without DOX treatment for 14 d and then analyzed as a control. *C*, Immunoblot analysis of EGFP/TeNT extinction in cerebellar lysates after withdrawal of DOX in mice pretreated with DOX for 14 d.

transgene showed the most intense signal of the GABA-α6/rtTA mRNA in the cerebellum (Fig. 2*A*). No such hybridization signal was observed in any other tissues nor in extracerebellar brain regions (Fig. 2*A*). *In situ* hybridization revealed that the GABA-α6/rtTA mRNA was restricted in the cerebellum and not present in any other brain regions (Fig. 2*B*). Furthermore, hybridization-positive grains were confined to granule cells and not observed in Purkinje cell layer, molecular layer, or white matter (Fig. 2*D,E*). In control, no hybridization signals were seen in any brain regions of wild-type mice (Fig. 2*C*).

Inducible and reversible expression of TeNT

Two independent founders of the TeNT mice were produced with four copies of the transgene. Heterozygous crossing between the TeNT (line 1317) and Tet (line 620) mice produced offspring of four different genotypes according to Mendel's rule. Administration of DOX was performed at ages of 4–5 weeks of the Tet/TeNT mice with 2 mg/ml DOX in drinking water and 6 mg/gm DOX in food pellets in all subsequent experiments (Fig. 3*A*; see timing protocol). After immunoblotting of cerebellar lysates of the Tet/TeNT mice (Fig. 3*B,C*), EGFP immunoreactivity was never observed in the DOX-untreated Tet/TeNT cerebellum (Fig. 3*B*). When DOX treatment was started, EGFP immunoreactivity became detectable from 3 d, increased to maximal levels on day 5, and kept this level as long as DOX was administered (Fig. 3*B*). When DOX was withdrawn after DOX treatment for 14 d, EGFP immunoreactivity in cerebellar lysates was reduced significantly on day 7 and decreased to undetectable levels on day 14 after DOX withdrawal (Fig. 3*C*). Consistent with the previous observation that TeNT has no effect on cell survival (Sweeney et al., 1995), the cell number, shape, and anatomical arrangement of the cerebellum were indistinguishable among the four genotypes (wild-type, Tet, TeNT, and Tet/TeNT mice), regardless of treatment with or without DOX as well as withdrawal after DOX treatment. These data demonstrate that the expression of EGFP/TeNT is regulated tightly in the cerebellum of the Tet/TeNT mice by DOX treatment.

Selective expression of TeNT in cerebellar granule cells

No GFP immunoreactivity was seen in cerebellar sections of either wild-type mice or DOX-untreated Tet/TeNT mice (Fig.

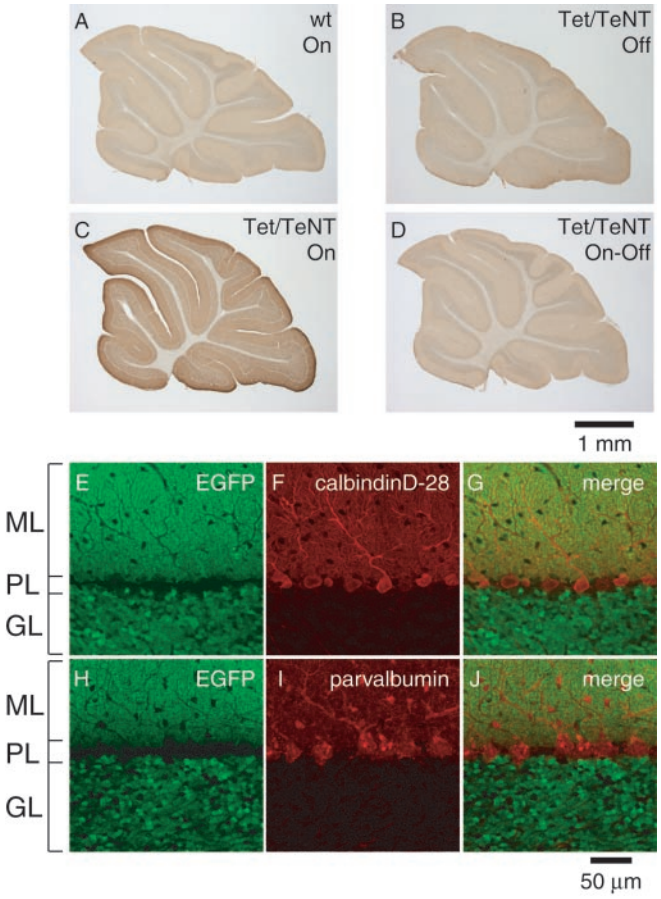

Figure 4. Immunohistochemical analysis of the TeNT expression. *A–D*, Sagittal sections of the cerebellum were immunostained with the GFP antibody. *A*, Wild-type mice (wt) treated with DOX for 7 d (On). *B*, DOX-untreated (Off) Tet/TeNT mice. *C*, Tet/TeNT mice treated with DOX for 7 d. *D*, Tet/TeNT mice for which DOX was withdrawn for 21 d after treatment of DOX for 14 d (On–Off). *E–J*, Sagittal sections of the cerebellum of DOX-treated Tet/TeNT mice were double immunostained with either GFP and calbindin D-28 antibodies (*E–G*) or GFP and parvalbumin antibodies (*H–J*). GFP immunoreactivity was seen at somata and axons of granule cells and was segregated completely from both calbindin D-28 immunoreactivity and parvalbumin immunoreactivity. ML, Molecular layer; PL, Purkinje cell layer; GL, granular layer.

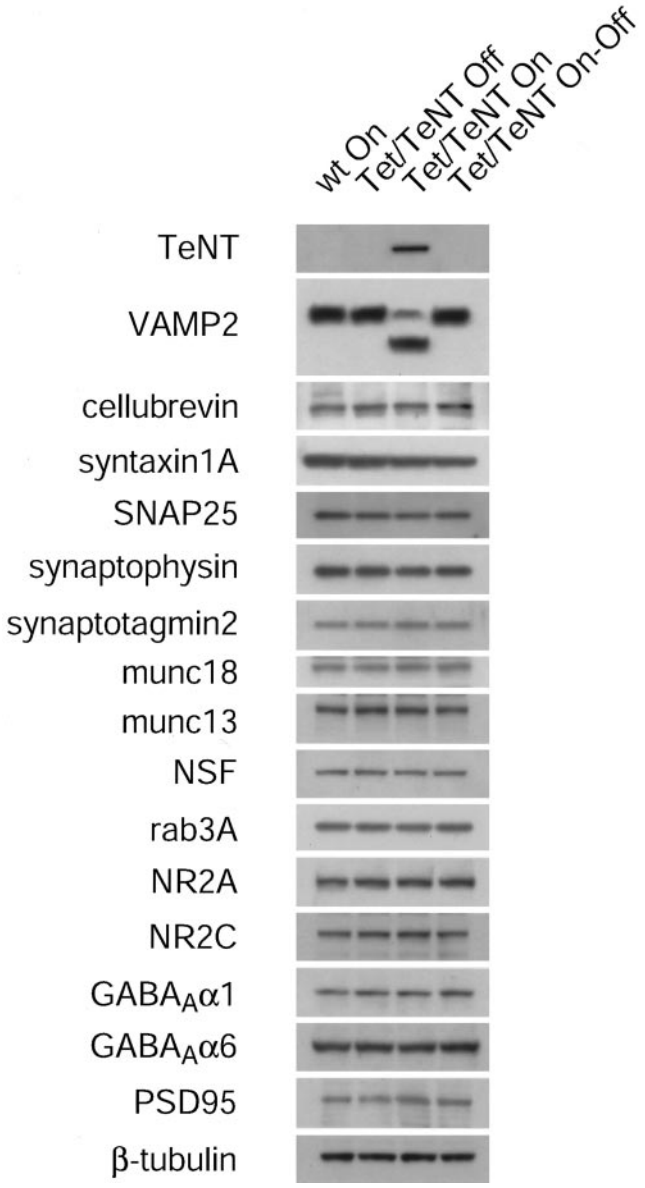

Figure 5. VAMP2 cleavage by TeNT expression in DOX-treated Tet/TeNT mice. Wild-type and Tet/TeNT mice were treated as indicated, and cerebellar lysates of these mice were immunoblotted with antibodies against TeNT, VAMP2, and 15 other proteins. VAMP2 was cleaved, but the other 15 proteins were not influenced by DOX-induced TeNT.

4*A*,*B*). When the Tet/TeNT mice were treated with DOX for 1 week, GFP immunoreactivity appeared at the molecular and granular layers, but not at the Purkinje cell layer or white matter (Fig. 4*C*). This immunoreactivity disappeared 3 weeks after DOX withdrawal in the Tet/TeNT mice pretreated with DOX for 2 weeks (Fig. 4*D*). The result indicates that the EGFP/TeNT protein is regulated selectively in a DOX-dependent manner also.

The restricted expression of EGFP/TeNT in cerebellar granule cells was examined further by double immunostaining either with GFP and calbindin D-28 antibodies or GFP and parvalbumin antibodies (Fig. 4*E–J*). Calbindin D-28 is a marker for Purkinje cells, whereas parvalbumin is a marker for basket, stellate, and Purkinje cells (Celio, 1990). GFP immunoreactivity was distributed in both somata of granule cells in the granular layer and their axons in the molecular layer (Fig. 4*E*,*H*). This immunoreactivity was segregated completely from both calbindin D-28 immunoreactivity (Fig. 4*E–G*) and parvalbumin immunoreactivity (Fig. 4*H–J*). The result explicitly indicates that EGFP/TeNT is induced selectively in cerebellar granule cells in the DOX-treated Tet/TeNT mice.

TeNT is a metalloprotease that cleaves 18 kDa VAMP2 between Glu-76 and phe-77 and produces the N-terminal 12 kDa and the C-terminal 6 kDa fragments (Schiavo et al., 1992). We examined whether DOX-induced TeNT results in cleavage of VAMP2 in the cerebellum by immunoblotting with the antibody against the N-terminal VAMP2 (Fig. 5). This analysis revealed that the intact 18 kDa VAMP2 was reduced greatly and cleaved to the 12 kDa N-terminal fragment in DOX-treated Tet/TeNT mice. This cleavage was never observed in wild-type, DOX-untreated, or DOX-withdrawn mice (Fig. 5). The partial cleavage observed for VAMP2 after DOX treatment may occur because of insufficient cleavage of VAMP2 by DOX-induced TeNT *in vivo*. However, the cerebellar lysates we analyzed also included TeNT-negative cell types. Therefore, it is also possible that intact VAMP2 is derived from the ubiquitously expressed VAMP2 in other TeNT-negative cell types (Trimble et al., 1990). The effects of DOX-induced TeNT on other neuronal proteins also were

analyzed by immunoblotting of cerebellar lysates with specific antibodies (Fig. 5). Neither changes in amounts of 15 representative proteins that were analyzed nor cleavage of these proteins was observed after induction of TeNT. More specifically, the VAMP2 homolog cellubrevin is known to be a target of TeNT cleavage (McMahon et al., 1993). However, no cleavage of cellubrevin was seen in DOX-treated Tet/TeNT mice, reflecting its expression in glial and vascular cells in the brain (Chilcote et al., 1995). The results demonstrate that the DOX-dependent induction of TeNT causes selective cleavage of VAMP2 in granule cells, but no compensatory changes nor degradation of the other proteins that were analyzed occurs in the Tet/TeNT mice after DOX treatment.

Reduction of glutamatergic transmission in TeNT-induced cerebellum

To examine whether the TeNT-mediated cleavage of VAMP2 reduces glutamatergic transmission at granule cell→Purkinje cell synapses, we first attempted whole-cell recording of Purkinje cell responses in slice preparations by electrically stimulating granule cell parallel fibers. However, under synaptic connections in which each Purkinje cell receives >100,000 parallel fibers (Napper and Harvey, 1988), glutamate released from a limited population of granule cells that contain intact VAMP2 still would be sufficient to induce excitation of a Purkinje cell. Because electrical stimulation of a defined number of parallel fibers was technically difficult, we found difficulty in quantifying electrophysiologically the effects of VAMP2 cleavage on glutamatergic transmission in slice preparations. We therefore measured changes of glutamate released from granule cells in cerebellar preparations. Cerebellar slices were prepared from wild-type, DOX-untreated, DOX-treated, and DOX-withdrawn Tet/TeNT mice. Glutamate release by depolarization with high KCl (25 mM) was measured by glutamate oxidase-immobilized reactor combined with HPLC (Fig. 6). Glutamate release was induced rapidly with the addition of high KCl and returned to basal levels with the washout (Fig. 6*A*). Under the nondepolarizing conditions, basal levels of glutamate release were unchanged among the four genotypes. After depolarization with high KCl, wild-type and DOX-untreated Tet/TeNT mice showed a marked increase in glutamate release with no statistical difference (Fig. 6). In contrast, glutamate release evoked by KCl depolarization was reduced greatly in DOX-treated Tet/TeNT mice, and this reduction was statistically significant as compared with both DOX-treated wild-type ($p < 0.01$) and DOX-untreated Tet/TeNT mice ($p < 0.05$; Fig. 6*B*). Furthermore, the reduction in glutamate release by DOX treatment recovered with the withdrawal of DOX ($p < 0.01$ as compared with DOX-treated Tet/TeNT mice; no statistical difference as compared with wild-type mice; Fig. 6*B*). These results demonstrate that glutamate release from granule cells is suppressed by DOX-induced TeNT and this impairment is recovered reversibly by the withdrawal of DOX.

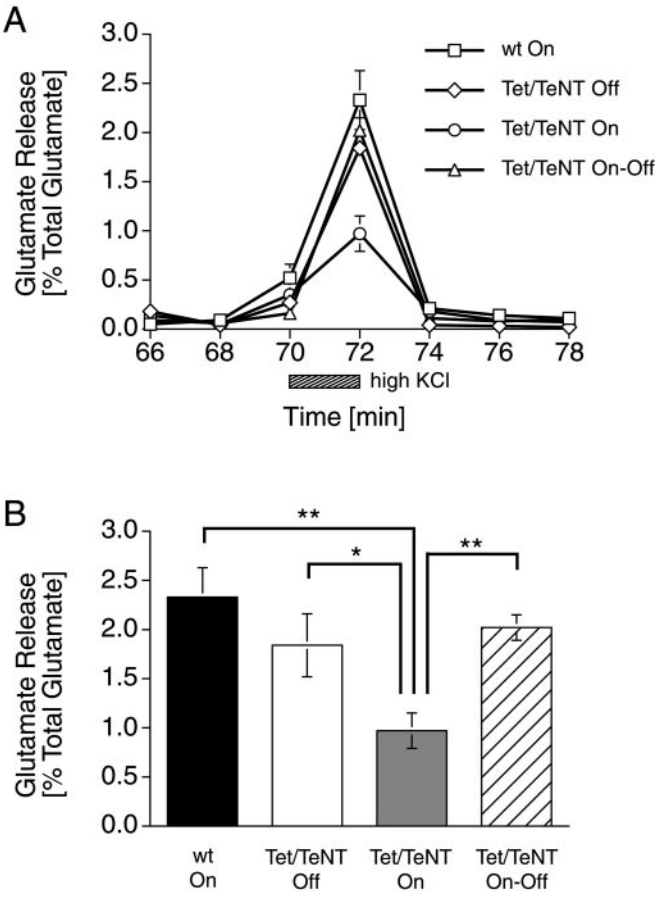

Figure 6. Quantification of KCl-evoked glutamate release. *A*, Wild-type and Tet/TeNT mice were treated with DOX as indicated, and cerebellar slices of these mice were prepared and incubated in the standard solution for 70 min. Then high KCl (25 mM) was superfused for 2 min, and released glutamate was collected. The ratio of glutamate released by KCl depolarization, relative to total glutamate in the superfusion and slice, was calculated and plotted against the time of slice incubation. Symbols and error bars indicate the mean ± SEM ($n = 5$ each). *B*, Histogram of KCl-evoked glutamate release at 72 min in *A*. Columns and error bars indicate the mean ± SEM (*$p < 0.05$ and **$p < 0.01$; $n = 5$ each; one-way ANOVA with Fisher's *post hoc* test).

Motor discoordination

The three transgenic mice (Tet, TeNT, and Tet/TeNT) walked normally on the ground, and none of them showed any ataxic gait or any sign of tremor, regardless of whether they were treated or untreated with DOX. Then the ability to adapt to challenging motor tasks was tested for the four genotypes (wild-type, Tet, TeNT, and Tet/TeNT) under three different conditions (DOX-untreated, DOX-treated, and DOX-withdrawn). We first performed a fixed bar test with the use of a narrow wooden bar. The wild-type, Tet, and TeNT mice could stand easily on the narrow bar under three conditions (Fig. 7*A–C*). The Tet/TeNT mice, when untreated with DOX, could manage this task comparably (Fig. 7*A*). However, when treated with DOX, the Tet/TeNT mice were unable to stand and crawled along the bar by grasping and pulling with their forepaws and dragging their hindlimbs. Furthermore, these mice fell off the bar more quickly than the others ($p < 0.01$; Fig. 7*B*). Importantly, this motor disorder of the Tet/TeNT mice recovered with the withdrawal of DOX (Fig. 7*C*).

We further characterized the motor discoordination with a rota-rod test, using a gritted roller (Fig. 7*D–F*). When the rota-rod was rotating at 35 rpm, all four DOX-untreated genotypes fell down immediately from the running roller at the first session but progressively improved this task by repeated trials. There was no statistical difference in every session among the four genotypes (Fig. 7*D*). When DOX was administered, the three genotypes (wild-type, Tet, and TeNT) showed comparable improvement with no statistical difference (Fig. 7*E*). In contrast, DOX-treated Tet/TeNT mice showed difficulty in managing this task, and the score achieved by these mice was reduced significantly (35.6–42.5%) as compared with other genotypes at the final session (Fig. 7*E*). Again, this motor impairment recovered to the levels of the three other genotypes when DOX was withdrawn for 3 weeks

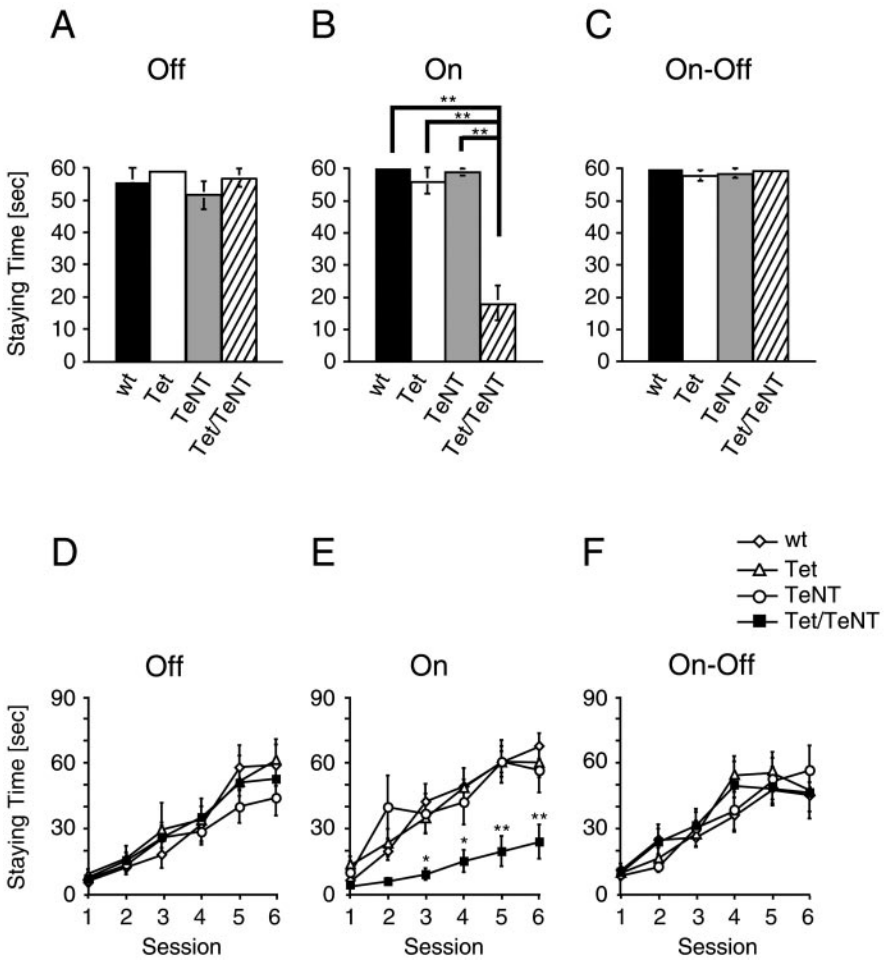

Figure 7. Fixed bar and rota-rod tests. *A–C*, The time mice remained on the 6-mm-wide bar was measured for a maximum of 60 sec. Mice were untreated with DOX in *A* and treated with DOX for 13 d in *B*. In *C*, DOX was removed for 21 d after mice received DOX for 14 d. Five to nine mice of each genotype were tested under three different experimental conditions. Columns and error bars indicate the mean ± SEM. The Tet/TeNT mice spent significantly less time on the bar than did other genotypes when treated with DOX (**$p < 0.01$; one-way ANOVA with Scheffé's *post hoc* test). No statistical difference was noted among wild-type, Tet, and TeNT mice when treated with DOX as well as among the four genotypes when DOX was untreated or withdrawn. *D–F*, The time an animal remained on a rota-rod rotated at 35 rpm was measured for six sessions. A maximum of 90 sec was allowed for each animal per session. Symbols and error bars indicate the mean ± SEM. Mice untreated (*D*) and treated with DOX for 13 d (*E*) are shown. *F*, DOX was removed for 21 d after treatment with DOX for 13 d. Five to 11 animals of each genotype were tested under three different experimental conditions. Repeated ANOVA showed that the Tet/TeNT mice stayed on the rota-rod for less time than did the other three genotypes when they were treated with DOX ($F_{(1,17)} = 27.8, p < 0.001$ vs wt; $F_{(1,19)} = 14.7, p < 0.002$ vs Tet; $F_{(1,17)} = 12.4, p < 0.003$ vs TeNT). All four genotypes remained on the rota-rod, with no statistical difference in *D* and *F*. In *E*, significant difference was noted when compared between DOX-treated Tet/TeNT and wild-type mice at each session (*$p < 0.05$ and **$p < 0.01$; one-way ANOVA with Scheffé's *post hoc* test).

(Fig. 7*F*). These results demonstrate that the motor coordination and discoordination are controlled reversibly by administration of DOX in the Tet/TeNT mice.

Discussion

In this study, we report a novel technique that allows reversible control of glutamatergic neurotransmission in specific neurons of living animals with spatiotemporal accuracy. This technique has been developed by genetic manipulation that combines the GABA-α6-directed expression of rtTA with the DOX/rtTA-controlled TeNT system.

The expression of the natural $GABA_A$ receptor α6 in wild-type mice is restricted but distributed in cochlear nucleus as well (Laurie et al., 1992; Varecka et al., 1994). Consistent with a previous report (Bahn et al., 1997), the GABA-α6 promoter we used was not functional in cochlear nucleus and further restricted the expression of the rtTA transgene in cerebellar granule cells. The GABA-α6 fragment that was used also encodes the extracellular ligand-binding domain and its following first transmembrane region of $GABA_A$ receptor α6 (Jones et al., 1996). The truncated GABA-α6 protein is nonfunctional as a GABA-gated ion channel (Davies et al., 1996; Xu and Akabas, 1996). Furthermore, an immunoreactive truncated form of GABA-α6 is not detectable in cerebellar lysates (data not shown), indicating that the truncated protein rapidly degrades as it is synthesized. In addition, Tet mice that have the ability to synthesize truncated GABA-α6 protein show no impairment in both glutamate release and motor coordination. It thus can be concluded that functional impairments of DOX-treated Tet/TeNT mice result from selective and reversible expression of TeNT in cerebellar granule cells.

Administration of TeNT to whole animals leads to animal death by respiratory movement failure because of impairment of synaptic transmission (Schiavo et al., 2000). When TeNT is expressed more widely in transgenic mice, spermatogenesis is impaired severely (Eisel et al., 1993). The VAMP2 homolog cellubrevin is involved in a more general exocytotic process (McMahon et al., 1993; Galli et al., 1994) and has been implicated in the effects of the widely expressed TeNT on spermatogenesis (Eisel et al., 1993). The null mutation of VAMP2, on the other hand, shows a lethal phenotype in mice immediately after birth (Schoch et al., 2001). In contrast, the Tet/TeNT mice grow normally and are viable after DOX treatment. Furthermore, these mice, even when treated with DOX, show a normal architecture with respect to the cell number, shape, and anatomical arrangement of granule cells and other cerebellar cells. These findings demonstrate that the developmental abnormality and lethality of TeNT are circumvented by the conditionally regulated spatiotemporal expression of TeNT.

In some cases, rtTA showed a leak expression of the transgene in the absence of DOX treatment (Kistner et al., 1996). This leak expression is thought to result from the positional effect because of integration of the transgene into the chromosome (Kistner et al., 1996) or a DOX-independent residual binding of rtTA to the TRE/CMV promoter (Urlinger et al., 2000). In the Tet/TeNT mice neither TeNT expression nor VAMP2 cleavage was observed in the absence of DOX treatment, and comparable glutamate release was induced in DOX-untreated Tet/TeNT mice as compared with wild-type mice. The TeNT expression thus was controlled tightly in the Tet/TeNT mice in a DOX-dependent manner. It has been reported that only 4–10 molecules of TeNT inhibited 50% of synaptic vesicle exocytosis in *Aplysia* (Mochida

et al., 1989; Schiavo et al., 2000). Therefore, care must be taken for application of the DOX/rtTA-controlled TeNT system, including use of restrictedly controlling promoter function and analysis of multiple independent founders of the Tet transgenic mice.

Recently, a temperature-sensitive dynamin mutant, *shibire*, was developed to control synaptic transmission reversibly in *Drosophila* on the time scale of minutes (Dubnau et al., 2001; McGuire et al., 2001). One limit of the DOX-inducing system is its slow kinetics in both activation and inactivation of neurotransmission regulation. In the TeNT transgene, the PEST sequence was attached to TeNT to facilitate its degradation, but the kinetics of induction and extinction of TeNT in our transgenic mice were comparable to those reported for the PEST sequence-lacking calcineurin that was controlled by the CaMKIIα promoter-directed rtTA (Mansuy et al., 1998). The uptake, distribution, and removal of DOX in the brain are potential determinants for pharmacokinetics of the DOX-inducing system. In addition, a high concentration of DOX is required to activate a low-affinity rtTA that we used (Gossen et al., 1995). Recently, a new version of a high-affinity rtTA such as rtTA2S-M2 has been developed (Urlinger et al., 2000). Use of this high-affinity rtTA could amend the requirement of a high concentration of DOX in the brain. Direct continuous perfusion of DOX into the brain also may improve pharmacokinetics of the DOX-inducing rtTA system, and this attempt is in progress to investigate the cerebellar function.

In the cerebellar cortex, Purkinje cells receive excitatory inputs from parallel fibers and climbing fibers and serve as the single output system (Ito, 1984). The reversible deficit of glutamatergic neurotransmission and its corresponding impairment of motor coordination demonstrate that the granule cell glutamatergic neurotransmission is critical in controlling motor coordination. The cerebellum also plays an important role in acquisition and maintenance of motor learning (Lisberger, 1988; Thompson and Krupa, 1994; Ito, 1998; Wolpert et al., 1998). Purkinje cells show long-term depression (LTD) by conjunctive stimulation of parallel fibers and climbing fibers (Ito et al., 1982). This long-lasting change in efficacy of synaptic transmission is thought to serve as a key mechanism for motor learning (Ito, 1989). However, many cellular components have been shown to involve the induction of LTD (Linden, 1994; Daniel et al., 1998), and the role and mechanisms of LTD in motor learning remain poorly understood. Whether and how the cerebellum participates in storage and retrieval of motor learning also remain to be clarified. Several behavioral models such as vestibulo-ocular reflex, optokinetics, and eyelid conditioning have been developed in mice to study the role and mechanisms of cerebellar function in motor learning (Aiba et al., 1994; Shibuki et al., 1996; De Zeeuw et al., 1998; Katoh et al., 2000). The manipulation of reversible cerebellar neurotransmission in the Tet/TeNT mice will help us to study the cerebellar function in the processes of acquisition, storage, and retrieval of motor learning.

References

Aiba A, Kano M, Chen C, Stanton ME, Fox GD, Herrup K, Zwingman TA, Tonegawa S (1994) Deficient cerebellar long-term depression and impaired motor learning in mGluR1 mutant mice. Cell 79:377–388.

Akazawa C, Shigemoto R, Bessho Y, Nakanishi S, Mizuno N (1994) Differential expression of five *N*-methyl-D-aspartate receptor subunit mRNAs in the cerebellum of developing and adult rats. J Comp Neurol 347:150–160.

Archer BT, Özçelik T, Jahn R, Francke U, Südhof TC (1990) Structures and chromosomal localizations of two human genes encoding synaptobrevins 1 and 2. J Biol Chem 265:17267–17273.

Bahn S, Jones A, Wisden W (1997) Directing gene expression to cerebellar granule cells using γ-aminobutyric acid type A receptor α6 subunit transgenes. Proc Natl Acad Sci USA 94:9417–9421.

Baumert M, Maycox PR, Navone F, De Camilli P, Jahn R (1989) Synaptobrevin: an integral membrane protein of 18,000 Daltons present in small synaptic vesicles of rat brain. EMBO J 8:379–384.

Celio MR (1990) Calbindin D-28K and parvalbumin in the rat nervous system. Neuroscience 35:375–475.

Chilcote TJ, Galli T, Mundigl O, Edelmann L, McPherson PS, Takei K, De Camilli P (1995) Cellubrevin and synaptobrevins: similar subcellular localization and biochemical properties in PC12 cells. J Cell Biol 129:219–231.

Daniel H, Levenes C, Crépel F (1998) Cellular mechanisms of cerebellar LTD. Trends Neurosci 21:401–407.

Davies M, Bateson AN, Dunn SMJ (1996) Molecular biology of the $GABA_A$ receptor: functional domains implicated by mutational analysis. Front Biosci 1:d214–d233.

De Zeeuw CI, Hansel C, Bian F, Koekkoek SKE, van Alphen AM, Linden DJ, Oberdick J (1998) Expression of a protein kinase C inhibitor in Purkinje cells blocks cerebellar LTD and adaptation of the vestibulo-ocular reflex. Neuron 20:495–508.

Dubnau J, Grady L, Kitamoto T, Tully T (2001) Disruption of neurotransmission in *Drosophila* mushroom body blocks retrieval but not acquisition of memory. Nature 411:476–480.

Eisel U, Reynolds K, Riddick M, Zimmer A, Niemann H, Zimmer A (1993) Tetanus toxin light chain expression in Sertoli cells of transgenic mice causes alterations of the actin cytoskeleton and disrupts spermatogenesis. EMBO J 12:3365–3372.

Elferink LA, Trimble WS, Scheller RH (1989) Two vesicle-associated membrane protein genes are differentially expressed in the rat central nervous system. J Biol Chem 264:11061–11064.

Galli T, Chilcote T, Mundigl O, Binz T, Niemann H, De Camilli P (1994) Tetanus toxin-mediated cleavage of cellubrevin impairs exocytosis of transferring receptor-containing vesicles in CHO cells. J Cell Biol 125:1015–1024.

Gogos JA, Osborne J, Nemes A, Mendelsohn M, Axel R (2000) Genetic ablation and restoration of the olfactory topographic map. Cell 103:609–620.

Gossen M, Freundlieb S, Bender G, Müller G, Hillen W, Bujard H (1995) Transcriptional activation by tetracyclines in mammalian cells. Science 268:1766–1769.

Hogan B, Beddington R, Costantini F, Lacey E (1994) Manipulating the mouse embryo: a laboratory manual, 2nd Ed. Cold Spring Harbor, NY: Cold Spring Harbor Laboratory.

Ito M (1984) The cerebellum and neural control. New York: Raven.

Ito M (1989) Long-term depression. Annu Rev Neurosci 12:85–102.

Ito M (1998) Cerebellar learning in the vestibulo-ocular reflex. Trends Cogn Sci 2:313–321.

Ito M, Sakurai M, Tongroach P (1982) Climbing fibre induced depression of both mossy fibre responsiveness and glutamate sensitivity of cerebellar Purkinje cells. J Physiol (Lond) 324:113–134.

Jackson RJ, Howell MT, Kaminski A (1990) The novel mechanism of initiation of picornavirus RNA translation. Trends Biochem Sci 15:477–483.

Jones A, Bahn S, Grant AL, Köhler M, Wisden W (1996) Characterization of a cerebellar granule cell-specific gene encoding the γ-aminobutyric acid type A receptor α6 subunit. J Neurochem 67:907–916.

Kadotani H, Hirano T, Masugi M, Nakamura K, Nakao K, Katsuki M, Nakanishi S (1996) Motor discoordination results from combined gene disruption of the NMDA receptor NR2A and NR2C subunits, but not from single disruption of the NR2A or NR2C subunit. J Neurosci 16:7859–7867.

Kaneko S, Hikida T, Watanabe D, Ichinose H, Nagatsu T, Kreitman RJ, Pastan I, Nakanishi S (2000) Synaptic integration mediated by striatal cholinergic interneurons in basal ganglia function. Science 289:633–637.

Katoh A, Kitazawa H, Itohara S, Nagao S (2000) Inhibition of nitric oxide synthesis and gene knockout of neuronal nitric oxide synthase impaired adaptation of mouse optokinetic response eye movements. Learn Mem 7:220–226.

Kistner A, Gossen M, Zimmermann F, Jerecic J, Ullmer C, Lübbert H, Bujard H (1996) Doxycycline-mediated quantitative and tissue-specific control of gene expression in transgenic mice. Proc Natl Acad Sci USA 93:10933–10938.

Kobayashi K, Morita S, Sawada H, Mizuguchi T, Yamada K, Nagatsu I, Fujita K, Kreitman RJ, Pastan I, Nagatsu T (1995) Immunotoxin-mediated conditional disruption of specific neurons in transgenic mice. Proc Natl Acad Sci USA 92:1132–1136.

Kozak M (1986) Point mutations define a sequence flanking the AUG initiator codon that modulates translation by eukaryotic ribosomes. Cell 44:283–292.

Laurie DJ, Seeburg PH, Wisden W (1992) The distribution of 13 $GABA_A$ receptor subunit mRNAs in the rat brain. II. Olfactory bulb and cerebellum. J Neurosci 12:1063–1076.

Li X, Zhao X, Fang Y, Jiang X, Duong T, Fan C, Huang C-C, Kain SR (1998) Generation of destabilized green fluorescent protein as a transcription reporter. J Biol Chem 273:34970–34975.

Linden DJ (1994) Long-term synaptic depression in the mammalian brain. Neuron 12:457–472.

Link E, Edelmann L, Chou JH, Binz T, Yamasaki S, Eisel U, Baumert M, Südhof TC, Niemann H, Jahn R (1992) Tetanus toxin action: inhibition of neurotransmitter release linked to synaptobrevin proteolysis. Biochem Biophys Res Commun 189:1017–1023.

Lisberger SG (1988) The neural basis for learning of simple motor skills. Science 242:728–735.

Lonart G, Janz R, Johnson KM, Südhof TC (1998) Mechanism of action of rab3A in mossy fiber LTP. Neuron 21:1141–1150.

Mansuy IM, Winder DG, Moallem TM, Osman M, Mayford M, Hawkins RD, Kandel ER (1998) Inducible and reversible gene expression with the rtTA system for the study of memory. Neuron 21:257–265.

McGuire SE, Le PT, Davis RL (2001) The role of *Drosophila* mushroom body signaling in olfactory memory. Science 293:1330–1333.

McMahon HT, Ushkaryov YA, Edelmann L, Link E, Binz T, Niemann H, Jahn R, Südhof TC (1993) Cellubrevin is a ubiquitous tetanus-toxin substrate homologous to a putative synaptic vesicle fusion protein. Nature 364:346–349.

Miyamoto Y, Yamada K, Noda Y, Mori H, Mishina M, Nabeshima T (2001) Hyperfunction of dopaminergic and serotonergic neuronal systems in mice lacking the NMDA receptor ϵ1 subunit. J Neurosci 21:750–757.

Mochida S, Poulain B, Weller U, Habermann E, Tauc L (1989) Light chain of tetanus toxin intracellularly inhibits acetylcholine release at neuroneuronal synapses, and its internalization is mediated by heavy chain. FEBS Lett 253:47–51.

Napper RMA, Harvey RJ (1988) Number of parallel fiber synapses on an individual Purkinje cell in the cerebellum of the rat. J Comp Neurol 274:168–177.

Nirenberg S, Cepko C (1993) Targeted ablation of diverse cell classes in the nervous system *in vivo*. J Neurosci 13:3238–3251.

Ohishi H, Ogawa-Meguro R, Shigemoto R, Kaneko T, Nakanishi S, Mizuno N (1994) Immunohistochemical localization of metabotropic glutamate receptors, mGluR2 and mGluR3, in rat cerebellar cortex. Neuron 13:55–66.

Oho C, Seino S, Takahashi M (1995) Expression and complex formation of soluble *N*-ethylmaleimide-sensitive factor attachment protein (SNAP) receptors in clonal rat endocrine cells. Neurosci Lett 186:208–210.

Schiavo G, Benfenati F, Poulain B, Rossetto O, Polverino de Laureto P, DasGupta BR, Montecucco C (1992) Tetanus and botulinum-B neurotoxins block neurotransmitter release by proteolytic cleavage of synaptobrevin. Nature 359:832–835.

Schiavo G, Matteoli M, Montecucco C (2000) Neurotoxins affecting neuroexocytosis. Physiol Rev 80:717–766.

Schoch S, Deák F, Königstorfer A, Mozhayeva M, Sara Y, Südhof TC, Kavalali ET (2001) SNARE function analyzed in synaptobrevin/VAMP knockout mice. Science 294:1117–1122.

Shibuki K, Gomi H, Chen L, Bao S, Kim JJ, Wakatsuki H, Fujisaki T, Fujimoto K, Katoh A, Ikeda T, Chen C, Thompson RF, Itohara S (1996) Deficient cerebellar long-term depression, impaired eyeblink conditioning, and normal motor coordination in GFAP mutant mice. Neuron 16:587–599.

Söllner T, Whiteheart SW, Brunner M, Erdjument-Bromage H, Geromanos S, Tempst P, Rothman JE (1993a) SNAP receptors implicated in vesicle targeting and fusion. Nature 362:318–324.

Söllner T, Bennett MK, Whiteheart SW, Scheller RH, Rothman JE (1993b) A protein assembly–disassembly pathway *in vitro* that may correspond to sequential steps of synaptic vesicle docking, activation, and fusion. Cell 75:409–418.

Steele PM, Medina JF, Nores WL, Mauk MD (1998) Using genetic mutations to study the neural basis of behavior. Cell 95:879–882.

Südhof TC (1995) The synaptic vesicle cycle: a cascade of protein–protein interactions. Nature 375:645–653.

Sweeney ST, Broadie K, Keane J, Niemann H, O'Kane CJ (1995) Targeted expression of tetanus toxin light chain in *Drosophila* specifically eliminates synaptic transmission and causes behavioral defects. Neuron 14:341–351.

Thompson RF, Krupa DJ (1994) Organization of memory traces in the mammalian brain. Annu Rev Neurosci 17:519–549.

Trimble WS, Gray TS, Elferink LA, Wilson MC, Scheller RH (1990) Distinct patterns of expression of two VAMP genes within the rat brain. J Neurosci 10:1380–1387.

Urlinger S, Baron U, Thellmann M, Hasan MT, Bujard H, Hillen W (2000) Exploring the sequence space for tetracycline-dependent transcriptional activators: novel mutations yield expanded range and sensitivity. Proc Natl Acad Sci USA 97:7963–7968.

Varecka L, Wu C-H, Rotter A, Frostholm A (1994) $GABA_A$/benzodiazepine receptor α6 subunit mRNA in granule cells of the cerebellar cortex and cochlear nuclei: expression in developing and mutant mice. J Comp Neurol 339:341–352.

Watanabe D, Inokawa H, Hashimoto K, Suzuki N, Kano M, Shigemoto R, Hirano T, Toyama K, Kaneko S, Yokoi M, Moriyoshi K, Suzuki M, Kobayashi K, Nagatsu T, Kreitman RJ, Pastan I, Nakanishi S (1998) Ablation of cerebellar Golgi cells disrupts synaptic integration involving GABA inhibition and NMDA receptor activation in motor coordination. Cell 95:17–27.

White BH, Osterwalder TP, Keshishian H (2001) Molecular genetic approaches to the targeted suppression of neuronal activity. Curr Biol 11:R1041–R1053.

Wolpert DM, Miall RC, Kawato M (1998) Internal models in the cerebellum. Trends Cogn Sci 2:338–347.

Xu M, Akabas MH (1996) Identification of channel-lining residues in the M2 membrane-spanning segment of the $GABA_A$ receptor α1 subunit. J Gen Physiol 107:195–205.

Yamamoto M, Takahashi H, Nakamura T, Hioki T, Nagayama S, Ooashi N, Sun X, Ishii T, Kudo Y, Nakajima-Iijima S, Kimchi A, Uchino S (1999) Developmental changes in distribution of death-associated protein kinase mRNAs. J Neurosci Res 58:674–683.

Yamamoto M, Hioki T, Ishii T, Nakajima-Iijima S, Uchino S (2002) DAP kinase activity is critical for C_2-ceramide-induced apoptosis in PC12 cells. Eur J Biochem 269:139–147.

Yao T, Suzuki S, Nishino H, Nakahara T (1995) On-line amperometric assay of glucose, L-glutamate, and acetylcholine using microdialysis probes and immobilized enzyme reactors. Electroanalysis 7:1114–1117.